ELECTRICAL ENGINEERING

Moisture-triggered physically transient electronics

Yang Gao,[1]* Ying Zhang,[2]* Xu Wang,[3]* Kyoseung Sim,[3]* Jingshen Liu,[4] Ji Chen,[4] Xue Feng,[5] Hangxun Xu,[2]† Cunjiang Yu[1,4,6]†

Physically transient electronics, a form of electronics that can physically disappear in a controllable manner, is very promising for emerging applications. Most of the transient processes reported so far only occur in aqueous solutions or biofluids, offering limited control over the triggering and degradation processes. We report novel moisture-triggered physically transient electronics, which exempt the needs of resorption solutions and can completely disappear within well-controlled time frames. The triggered transient process starts with the hydrolysis of the polyanhydride substrate in the presence of trace amounts of moisture in the air, a process that can generate products of corrosive organic acids to digest various inorganic electronic materials and components. Polyanhydride is the only example of polymer that undergoes surface erosion, a distinct feature that enables stable operation of the functional devices over a predefined time frame. Clear advantages of this novel triggered transience mode include that the lifetime of the devices can be precisely controlled by varying the moisture levels and changing the composition of the polymer substrate. The transience time scale can be tuned from days to weeks. Various transient devices, ranging from passive electronics (such as antenna, resistor, and capacitor) to active electronics (such as transistor, diodes, optoelectronics, and memories), and an integrated system as a platform demonstration have been developed to illustrate the concept and verify the feasibility of this design strategy.

INTRODUCTION

The substantial and increasing demands for the prevention of sensitive data leakage, the reduction of electronic waste, or the elimination of second surgery to remove electronic implants suggest the need for electronics able to disappear physically in a controlled manner. Recent advances in transient electronics have paved the way for such devices (*1*–*5*). Examples include electrophysiological sensors (*5*), diagnostic brain implants as well as therapeutic implants for therapizing and biosensing (*2*), degradable microwave electronics (*4*) toward applications in temporal medical implants (*2*, *6*), disposable sensors (*5*, *7*, *8*), data-secure hardware systems (*9*–*11*), and environment-friendly degradable devices (*4*). However, most of the transient electronics achieve their transience through chemical dissolution with the device submerged in aqueous solutions or biofluids (*1*, *3*, *6*, *7*, *12*–*22*), with little control over the transience period, where the transience is passively governed by chemical dissolution or mechanical destruction of the functional devices associated with the degradation process. In addition, materials limited to biofluidic resorption or degradation, such as inorganic semiconductors (for example, Si) (*23*), metal conductors (for example, Mg, Mo, W, Zn, and Fe) (*24*), insulators (for example, MgO, SiO_2, and Si_3N_4) (*1*, *20*), and encapsulation layers or substrates [for example, silk fibroin, poly(lactic acid), poly(ε-caprolactone), and poly(vinyl alcohol)] (*1*, *21*, *22*, *25*), have been chosen to construct transient electronics. A collection of other materials, such as Cu, Ni, and Al, are typically excluded because they are undissolvable under these conditions.

Here, we report a new type of physically transient electronics whose transience mode is triggered by moisture, which is common yet challenging to be applied in transient electronics, constructed in the format of functional devices on top of hydrolytically liable polyanhydride substrates; this design exempts the needs of resorption solutions, and the electronics can completely disappear after a controllable time period. The transient process is attributed to the hydrolysis of the polyanhydride substrate in the presence of trace amounts of water molecules in the air, a process that can generate corrosive organic acids to digest various inorganic electronic materials and components, such as metal electrodes, metal oxide dielectrics, and semiconductors. This unique transience chemistry ensures complete degradation of entire electronic devices in air (Fig. 1A) and broadens our selection of materials suitable for constructing transient electronics. The lifetime of the moisture-triggered transient devices can be precisely controlled by varying the humidity level in the surrounding environment or by changing the substrate compositions, a distinct feature that enables stable operation of the devices over a predefined time frame. The moisture-triggered physically transient electronics have several distinct advantages: (i) The degradation kinetics or transient behaviors can be tuned by varying the polymer compositions or moisture levels; (ii) the devices can maintain stable operation until the polyanhydride is triggered to hydrolyze; (iii) polyanhydride undergoes a surface erosion process, and nearly no associated mechanical strain will be imposed onto the functional devices (*26*, *27*); and (iv) organic acids generated during the hydrolysis process can dissolve a wide range of electrode materials, semiconductors, and dielectrics that are typically considered to be nontransient. The associated materials, device designs, and fabrication methods described here could possibly lead to the development of eco-friendly disposable electronics and sensors, weapons, and explosives, which are expected to function for only a certain time period and then physically disappear.

[1]Department of Mechanical Engineering, University of Houston, Houston, TX 77204, USA. [2]Department of Polymer Science and Engineering, CAS (Chinese Academy of Science) Key Laboratory of Soft Matter Chemistry, University of Science and Technology of China, Hefei, Anhui 230026, China. [3]Materials Science and Engineering Program, University of Houston, Houston, TX 77204, USA. [4]Department of Electrical and Computer Engineering, University of Houston, Houston, TX 77204, USA. [5]Department of Engineering Mechanics, Center for Advanced Mechanics and Materials, Tsinghua University, Beijing 100084, China. [6]Department of Biomedical Engineering, University of Houston, Houston, TX 77204, USA.
*These authors contributed equally to this work.
†Corresponding author. Email: hxu@ustc.edu.cn (H.X.); cyu15@uh.edu (C.Y.)

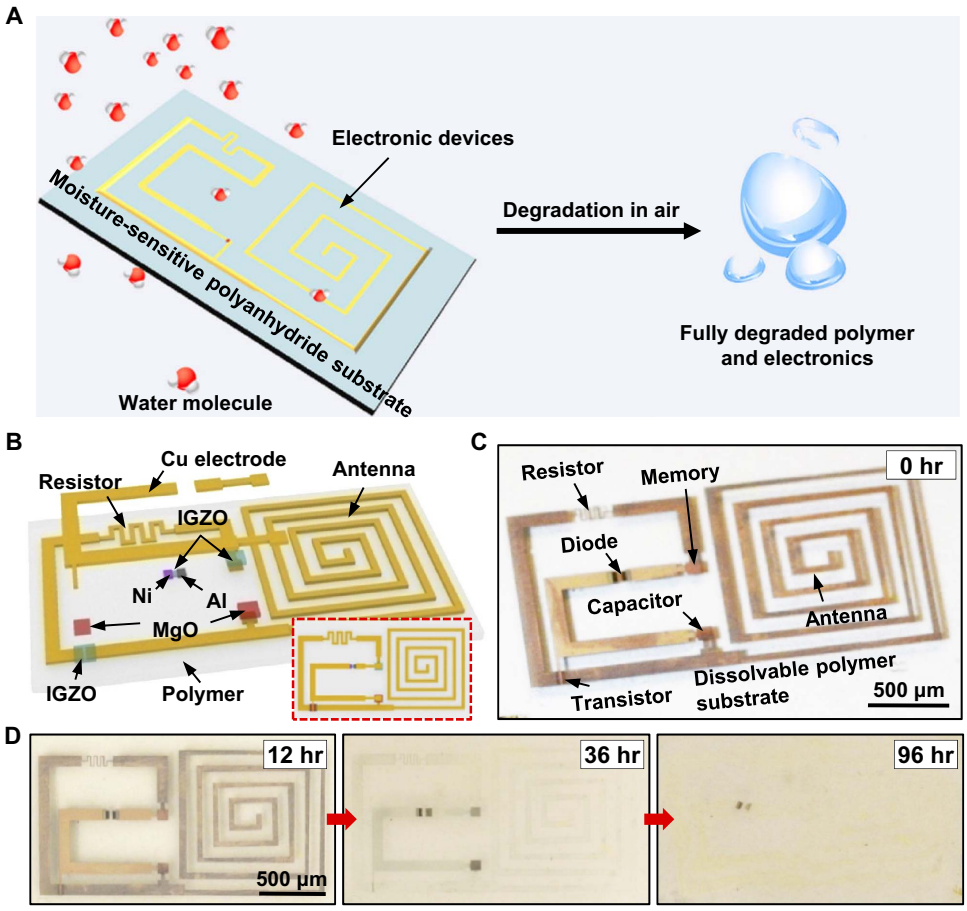

Fig. 1. Moisture-triggered physically transient electronics: A demonstration platform. (**A**) Schematic illustration of the moisture-triggered transience of the demonstration platform. (**B**) Explored illustration of an integrated electronics that includes a transistor, a diode, a memory, a capacitor, an antenna, and a resistor, with interconnects and dielectrics on a moisture-sensitive degradable polymer substrate. The inset in the lower right of the figure shows the top view. (**C**) Optical image of the circuit fabricated on the substrate. (**D**) Optical images showing the time-sequential dissolution of the device under 75% relative humidity.

RESULTS

Demonstration of a moisture-triggered transient electronic system

The humidity-controlled transient electronics are constructed on a polyanhydride substrate through multiple steps of additive microfabrication processes. A demonstration platform, schematically illustrated in Fig. 1B, consists of an antenna, a capacitor, a resistor, a diode, a transistor, a unit cell of a resistive memory, interconnects, and the polyanhydride substrate (Fig. 1C). Specifically, Cu was used as the conductors and electrodes for the transistor, the capacitor, and the resistive memory. Ni and Al were chosen as the electrodes for the diode to form Schottky and ohmic contacts, respectively. The semiconductor indium gallium zinc oxide (IGZO) was used to construct the transistor, the diode, and the resistive memory. Magnesium oxide (MgO) was used as an insulating dielectric for the transistor and the capacitor. The fabrication of the device involves direct deposition of multiple materials through Kapton film–based shadow masks. The details can be found in the Supplementary Materials. The transient characteristics of this demonstration platform under a relative humidity of 75% are illustrated by the sequential time elapse optical images in Fig. 1D. These results clearly indicate that the design strategy for moisture-triggered transient electronics is feasible.

Moisture-triggered hydrolysis of polyanhydride substrates

The polyanhydride substrate was synthesized by photochemical cross-linking of 4-pentenoic anhydride, poly(ethylene glycol) (PEG) diacrylate, and pentaerythritol tetrakis(mercaptoacetate) (Fig. 2A). The detailed synthetic procedures can be found in Materials and Methods. Here, the thickness of the polymer substrates used for all transient electronic devices is controlled at ~124 μm (fig. S1). The transmittance of the polymer substrate is more than 90% in the visible spectrum region (400 to 700 nm) (fig. S2). Besides in aqueous solutions, hydrolysis of polyanhydride can occur in air where moisture exists. The chemical reaction responsible for the hydrolysis of the polymer is illustrated in Fig. 2A. In particular, the polyanhydride undergoes a surface erosion process rather than expanding globally for other degradable polymers (*28*), and therefore, nearly no associated mechanical strain will be imposed onto the integrated functional devices. The polymer can absorb moisture in the air, and the anhydride groups react with the absorbed water molecules to trigger the hydrolysis process. The Fourier transform infrared (FTIR) spectroscopy results (Fig. 2B) show that the characteristic stretching vibration peak of C=O in anhydride group around 1814 cm^{-1} disappeared after hydrolysis for 72 hours under ~90% humidity, clearly indicating the hydrolysis of anhydride groups. In addition, a new peak due to the

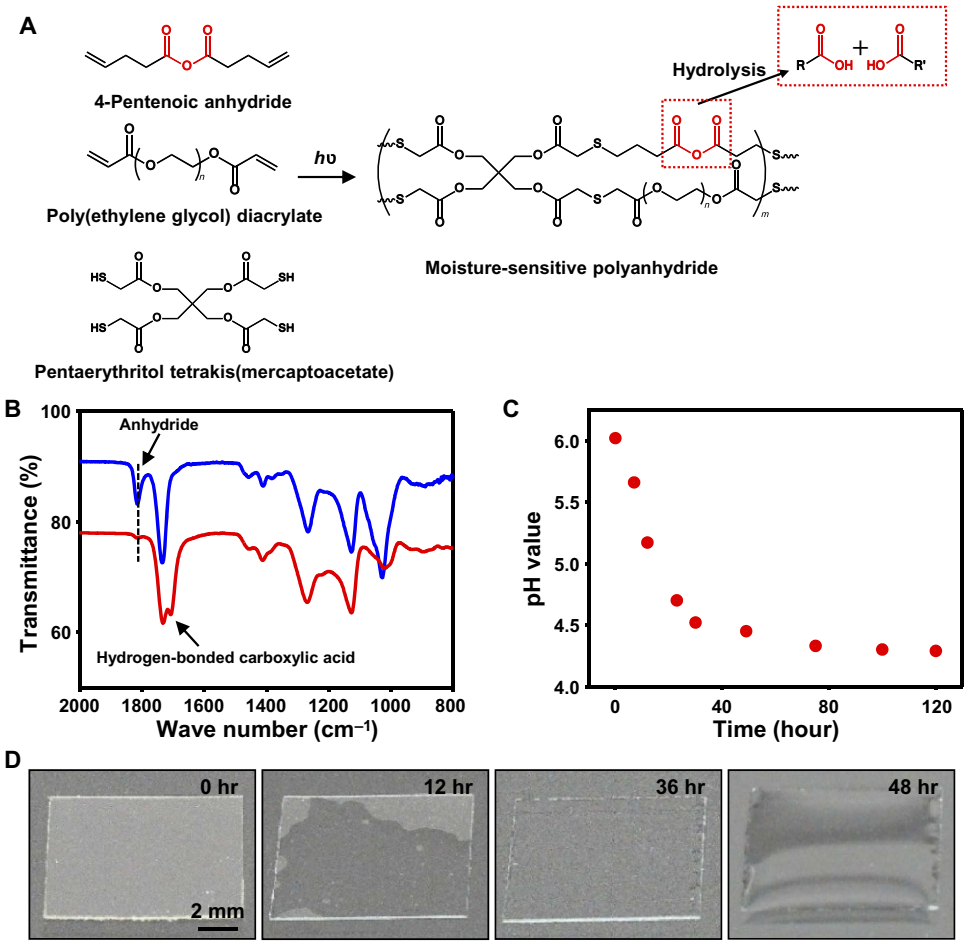

Fig. 2. Moisture-triggered degradation of the polyanhydride films. (**A**) Ultraviolet (UV) light–initiated synthesis of the polyanhydride thin films with the moisture-sensitive anhydride group, which can hydrolyze into organic acids with moisture. (**B**) FTIR spectra of the polymer before and after the hydrolysis process. (**C**) The time-sequential change of pH values of the polyanhydride polymer with 10% PEG during the hydrolysis process occurring in water. (**D**) Optical images showing the time-sequential hydrolysis of the polymer with 10% PEG.

hydrogen-bonded form of carboxylic acid at 1708 cm^{-1} appeared, further confirming the formation of carboxylic acid after hydrolysis of anhydride groups with moisture. When the humidity is controlled to be 0%, no variations could be observed from the FTIR spectra (fig. S3), indicating that no hydrolysis can occur. We also examined the change of pH values when 28 mg of polyanhydride containing 10% (molar ratio) PEG was added into 10 ml of pure water. As shown in Fig. 2C, the pH value decreased from 6.0 to 4.3 after 120 min, implying that acids were generated after the hydrolysis reaction. As hydrolysis proceeds, the solid polyanhydride thin film turned into a viscous liquid, as seen in Fig. 2D. This solid-to-liquid phase change is sometimes highly desirable for transient electronics because the fully degraded products can be easily washed away with water (*1*).

Furthermore, the degradation processes of the polymer thin film are tunable with different polymer compositions and different levels of humidity. By increasing the content of the anhydride, that is, decreasing the content of PEG (see the Supplementary Materials for details), the polyanhydride hydrolysis speeds up, and it takes less time to realize complete hydrolysis. Meanwhile, at a fixed relative humidity of 90%, the polyanhydride substrates with PEG content of 0 and 10% took 36 and 48 hours to completely turn into viscous liquids, whereas those with 20 and 30% of PEG were partially (about 50%) hydrolyzed after 48 and 96 hours, respectively. However, for the one with PEG content of 50%, only slight hydrolysis was observed even after 96 hours. By decreasing the relative humidity, the hydrolysis speed slows down. The detailed hydrolysis results for polyanhydrides with different PEG compositions and different film thicknesses under different relative humidity levels are presented in figs. S4 to S7. Overall, the time scale of complete hydrolysis can be tuned from days to weeks. It is noted that in this work, we mostly chose the polyanhydrides with high-content anhydride groups and made the transient process of the materials and devices relatively fast to illustrate the concept and to meet the relative short transient period needs after triggering in broad applications.

Moisture-triggered degradation of electronic materials

The corrosive nature of the acids generated during hydrolysis is applicable to a very broad range of electronic materials. Here, metals (for example, Cu, Ni, and Al), semiconductors (for example, IGZO), and insulating dielectrics (for example, MgO) were specifically used to build the physically transient devices. Figure 3A captures the associated chemical reactions. With this unique degradation mechanism, a wide collection of materials without transient properties in aqueous solutions are suitable for constructing transient electronics. Figure 3

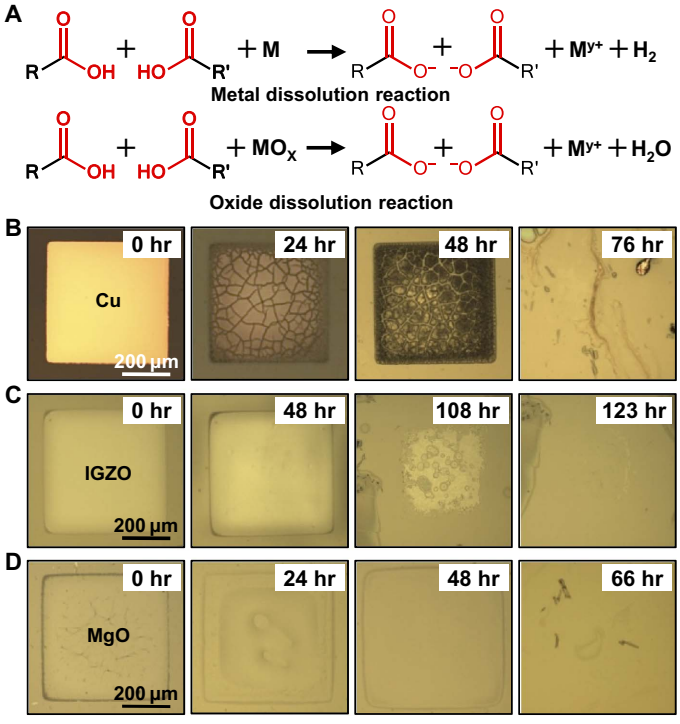

Fig. 3. Dissolution kinetics of core materials used in the moisture-triggered transient devices. (**A**) Chemical reactions responsible for triggered transience of metals and oxides. (**B**) Optical images showing the time-sequential dissolution of the Cu membrane. (**C**) Optical images showing the time-sequential dissolution of the IGZO membrane. (**D**) Optical images showing the time-sequential dissolution of the MgO membrane.

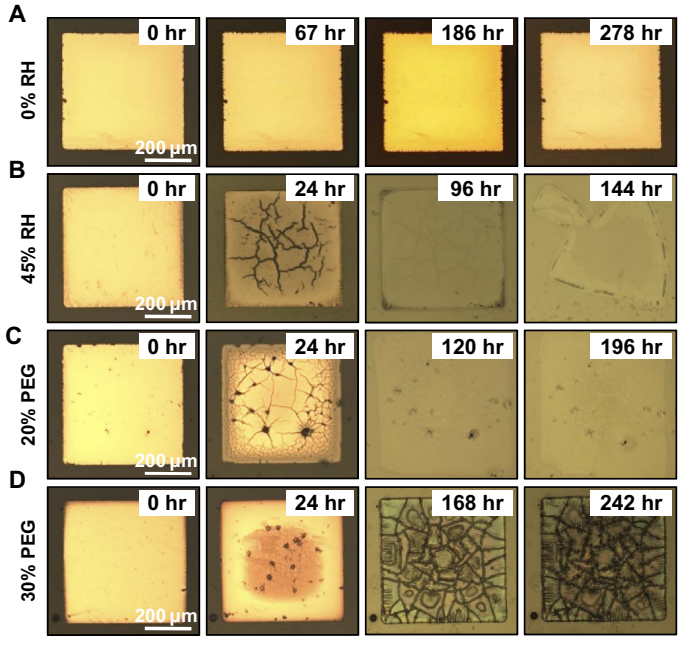

Fig. 4. Controlled transience process by controlling the environmental humidity levels and the polymer compositions. (**A** and **B**) Optical images showing the time-sequential dissolution of the Cu membranes under relative humidity (RH) of 0 and 45%, respectively. (**C** and **D**) Optical images showing the time-sequential dissolution of the Cu membranes on the polymer substrates with 20 and 30% PEG, respectively, under a relative humidity of 75%.

(B to D) shows the time-sequential images of dissolution for Cu, IGZO, and MgO thin membranes (500 × 500 μm^2, 50 nm thick) under a relative humidity of ~75%. All these materials completely degraded after about 5 days. The hydrolysis of the polymer substrates and thus the amount of acids generated can be tuned by controlling the environmental conditions, that is, humidity. As a result, the degradation kinetics of the electronic materials can be well controlled. The time-sequential images in Figs. 3B and 4 (A and B) verify that the Cu thin membrane (500 × 500 μm^2, 50 nm thick) exhibited different dissolution kinetics under different humidity levels. Under extremely dry conditions with a humidity of nearly 0%, no significant changes can be observed from the Cu thin film (Fig. 4A). Meanwhile the Cu thin membrane completely degraded within 144 hours at a relative humidity of 45% (Fig. 4B) and 76 hours at a relative humidity of 75% (Fig. 3B). The effect of anhydride contents of the polyanhydride substrates on the degradation behaviors of the electronic materials was also carefully examined. Cu thin membranes on different substrates (Figs. 3B and 4, C and D) exhibited different degradation kinetics. Obviously, higher content of the anhydride groups in the polymer substrate leads to more efficient degradation, which is consistent with the hydrolysis kinetics of the polyanhydride substrate as described previously.

Moisture-triggered degradation of electronic devices

The broadened range of suitable electronic materials and the established fabrication techniques allow us to design and fabricate a variety of electronic devices and potential functional systems. Therefore, we constructed a set of passive and active electronic devices in the moisture-triggered transient format. The dissolution behaviors of these devices were studied using polyanhydride substrates with 10% PEG. All the degradation processes were carried out under a humidity of 75%. Figure 5 presents the moisture-triggered transience of passive devices, including the resistor, the antenna, and the capacitor, based on Cu and MgO. As shown in Fig. 5 (A and B), as the hydrolysis of the polymer substrates started, the Cu resistor started to be eroded, as evidenced by the increase of the resistance (continuously monitored between the contact pads). Specifically, the resistance increased from 600 to 1000 ohms within 20 hours. Upon further hydrolysis, the resistance increased markedly, reaching 10 megohms at ~25 hours, where many cracks appeared and discontinued the electrical current path.

Figure 5C presents the sequential time elapse images of a Cu antenna on a polyanhydride substrate. The characteristics of the antenna during the transience were captured, as illustrated in Fig. 5D. The detailed sample dimensions and measurement setup are shown in fig. S8. The S11 of the antenna had a resonance at 3.1 GHz. As the transience process began, the resonance frequency of the antenna showed a slight shift. However, upon further degradation, a significant shift was observed. The current path on the antenna was influenced by the dissolution, and we noticed that the S11 magnitude curve shifted to a lower frequency. After 168 hours, the antenna was mostly dissolved and completely disintegrated. No antenna characteristic was obtained according to the measured S11 results.

The time elapse images of the transience process of a metal-insulator-metal structured capacitor (fig. S9, A to C) array are shown in Fig. 5E, in which Cu served as the top and bottom electrodes and MgO as the dielectric. The measured capacitance before the transience is shown in fig. S9D. At a frequency range of 0.1 to 100 kHz,

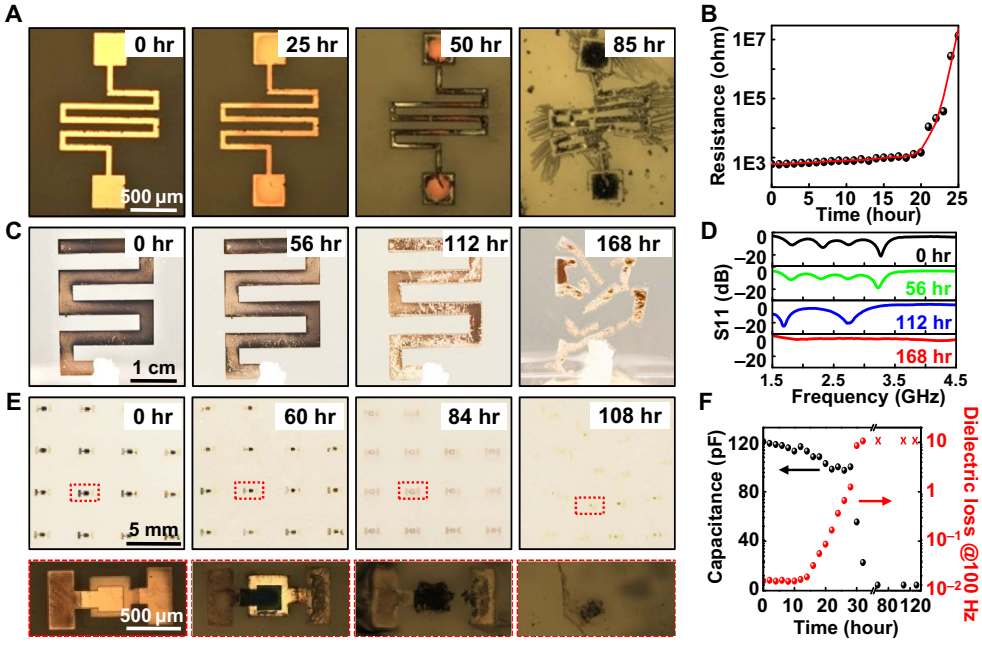

Fig. 5. Moisture-triggered transience of passive devices. (**A**) Optical images showing the time-sequential dissolution of a resistor. (**B**) Measured transience of a resistor. (**C**) Optical images showing the time-sequential dissolution of an antenna. (**D**) Measured transience of the antenna. (**E**) Optical images showing the time-sequential dissolution of the capacitor, with the top row showing the dissolution of a 4 × 4 array of capacitors. The bottom frames are the magnified images. (**F**) Measured transience of the capacitance and dielectric loss of the transient capacitor.

the device has a capacitance of ~125 pF. The capacitors disappeared after 108 hours. Figure 5F presents the measured transient characteristics of the capacitance and dielectric loss of the transient capacitor at a frequency of 100 Hz.

Figure 6 presents the moisture-triggered transience of active devices, including arrays of thin-film transistors (TFTs), logic gates, diodes, photodetectors, and resistive memories. The transistors used IGZO, MgO, and Cu as the n-type semiconductor, gate dielectrics, and metal electrodes for source, drain, and gate, respectively (fig. S10, A to C). The channel length and width were designed to be 80 and 300 μm, respectively. The details of the device structure are shown in Fig. 6A (optical image) and fig. S10A (schematic illustration). Figure 6B and fig. S10D show the output and transfer curves of the TFT, respectively. The TFTs demonstrated an n-type behavior, with a field effect mobility of 6.98 $cm^2/V{\cdot}s$, an on/off ratio of 7.93×10^4, a threshold voltage of 13.21 V, and a subthreshold swing of 1.14 V/decade. The performance of this device on the polyanhydride substrates is comparable to the counterpart on a rigid wafer (*4*, *29*). Figure 6A shows the time elapse images of the transience process of the transistors, and the array almost completely disappeared after 72 hours. The measured transience characteristics of the TFT, that is, the transfer curves over the transience period, are illustrated in Fig. 6C. The current decreases over time, and eventually, no current can be extracted after about 40 hours.

The inverters, that is, logic gates, used the same materials as those for the transistors (fig. S11). On the basis of two IGZO transistors, an NMOS inverter with an enhancement load was fabricated with channel widths of 100 and 300 μm for load and driver transistors, respectively. The optical image of the device is exhibited in Fig. 6D. Figure 6E shows the measured voltage transfer curve and gain of the inverter, while the V_{DD} was kept at 20 V. The inverter has a voltage gain of 1.03. Figure 6D shows the time elapse images of the transience process of the inverters, and the devices almost completely disappeared after 72 hours. Once the transience process starts, the output voltage at an input voltage of 0 V decreases over time, as illustrated in Fig. 6F.

The Schottky diodes used IGZO (conduction band E_{CB} ~ 4.5 eV) (*30*) as the active material. Ni (ϕ ~ 5.35 eV) (*31*) and Al (ϕ ~ 4.2 eV) (*32*) electrodes were chosen to form a Schottky contact and an ohmic contact with the IGZO, respectively. The device array and detailed structures are illustrated in Fig. 6G and fig. S12, respectively. A typical rectifying characteristic of the *I-V* curve is shown in Fig. 6H. Figure 6G shows the sequential time elapse images of the transience process of the diodes, and the devices almost completely disappeared after 93 hours. During the dissolution process, the transient current decreases, as demonstrated in Fig. 6 (H and I). Eventually, the device becomes disconnected with no detectable current.

The photodetectors (Fig. 6J) were fabricated using IGZO as the active material and Cu as the metal electrodes, as schematically illustrated in fig. S13. The photoresponse of the photodetector is shown in Fig. 6K. At 20-V bias, the photocurrents under illumination and in the dark are 0.48 μA and 7.2 nA, respectively. The calculated current ratio under illumination and in the dark is ~66.7 at 20-V bias, based on the equation $R = I_{bright}/I_{dark}$. Figure 6J shows the time elapse images of the transience process of the photodetectors, and the devices almost completely disappeared after 72 hours. Both the current in the dark and that under illumination under the bias of 10 V decrease after the hydrolysis starts, as illustrated in Fig. 6L.

Memory devices for future data storage purposes were also demonstrated. The left panel of Fig. 6M shows a 4 × 4–arrayed resistive memory device. The device was constructed using IGZO and Cu as the active material and metal electrodes, respectively. The detailed design of the device is shown in fig. S14 (A to C). Figure 6N shows the measured *I-V* curves of the memory device before transience happened. The device initially showed a high-resistance state. After the application of a positive voltage ("SET" at 1.67 V), the high-resistance state

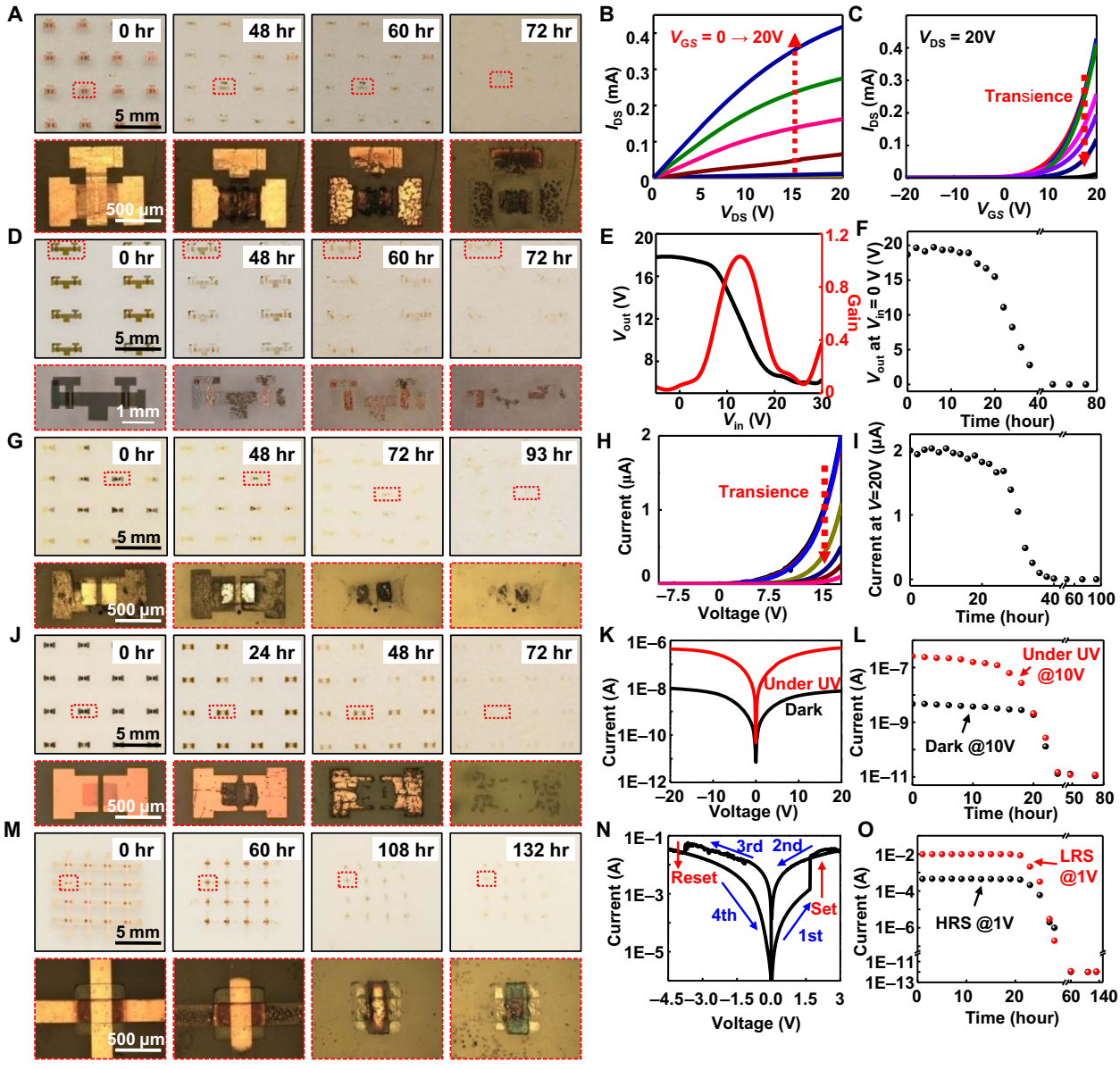

Fig. 6. Dissolution behaviors of the active devices of the moisture-triggered transient devices. (**A**) Optical images showing the time-sequential dissolution of the TFTs. The bottom frames are the magnified images. (**B**) Measured current-voltage (*I-V*) characteristics of a TFT before transience starts. (**C**) Measured transience of the transfer curves of the TFT. (**D**) Optical images showing the time-sequential dissolution of the logic gates. The bottom frames are the magnified images. (**E**) Measured voltage transfer curve and gain of the inverter before transience starts. (**F**) Measured transience of the output voltage of the inverter at V_{in} = 0 V. (**G**) Optical images showing the time-sequential dissolution of the diodes. The bottom frames are the magnified images. (**H**) Measured *I-V* curves of a diode before and after transience starts. (**I**) Measured transience of the current of a diode at V = 20 V. (**J**) Optical images showing the time-sequential dissolution of the photodetectors. The bottom frames are the magnified images. (**K**) Measured *I-V* curve of photodetector under UV and in the dark before transience starts. (**L**) Measured transience of the current of the photodetector at V = 10 V under UV and in the dark. (**M**) Optical images showing the time-sequential dissolution of the resistive memories. The bottom frames are the magnified images. (**N**) *I-V* characteristics of a resistive memory before transience starts. (**O**) The measured transience of the current of the resistive memory at V = 1 V at low-resistance state (LRS) and high-resistance state (HRS).

switched to a low-resistance state. By applying a negative voltage ("RESET" at −3.75 V), the low-resistance state switched back to the high-resistance state. The reliability of the IGZO memory device was studied, as shown in fig. S14 (D and E). Before the transience process started, the device maintained its characteristics without obvious degradation after continuous sweeping for 1000 s, and stable write-read-erase-read cycles were obtained. The time elapse images of the transience process of the resistive memory device are shown in Fig. 6M. The device took about 132 hours to dissolve. Once the transience process starts, the measured electrical current at both low-resistance state and high-resistance state experiences a slow drop in the first 24 hours and then a fast drop afterward before the device completely malfunctions. These results on moisture-triggered transience of various electronic devices lay the solid foundation of constructing sophisticated integrated functional systems, including but not limited to the one illustrated in Fig. 1.

DISCUSSION

In conclusion, we demonstrate that polymeric substrates with novel degradation kinetics and associated transience chemistry offer a feasible strategy for constructing physically transient electronics. Through the manipulation of the polymer component and environmental humidity, the progress of hydrolyzing polyanhydrides can be managed, and thus, the dissolution kinetics of functional device can be controlled. The transience time scale can be tuned from days to weeks, and even a wider time span if needed. The moisture-triggered physically transient electronics in this work represents a novel class of transient electronics featuring controllable degradation of the polymer substrates and functional electronics and a broadened selection of electronic materials. With the successful demonstration of various transient devices, ranging from passive components to active electronics, and an integrated system demonstration, we expect that this triggered transient mode can be applicable for future transient electronic systems, which may include a combined set of integrated circuit, sensors, data storage, signal transmission, etc.

MATERIALS AND METHODS

Synthesis of moisture-sensitive polyanhydride thin films

To prepare the polyanhydride substrates, for instance with 10% PEG (molar ratio), 4-pentenoic anhydride (131.2 mg; 0.72 mmol), PEG diacrylate (20 mg; 0.08 mmol), pentaerythritol tetrakis(mercaptoacetate) (173 mg; 0.4 mmol), and 2,2-dimethoxy-2-phenylacetophenone (3 mg; 0.012 mmol) were firstly mixed in a 5-ml vial. Then, vortex mixing and ultrasonication were used to help dissolve all of the components. After the bubbles were removed, the mixture solution became homogeneous. A syringe was used to slowly inject the mixture into a mold, and the thickness of the film was controlled by the volume of the solution. The polyanhydride thin films were obtained after polymerization under a UV curing lamp (model 234100, Boekel Scientific Inc.) for 5 min. Moisture-triggered degradable polyanhydride thin films with different hydrolyzing kinetics can be obtained by varying the contents of PEG in the precursor solutions.

Shadow mask preparation

The shadow masks were made of 25.4-μm-thick polyimide film (Kapton film, DuPont). The preparation of shadow mask began with coating a thin layer of polydimethylsiloxane (PDMS) on a cleaned glass slide and curing to form an adhesive layer. A piece of Kapton film was carefully laminated onto the PDMS surface and dehydrated at 90°C for 10 min after cleaning the film surface. Thereafter, a layer of 500-nm-thick Cu was deposited on top of the polyimide film using electron-beam (e-beam) evaporation, followed by patterning through photolithography and wet etching to pattern the Cu. Reactive ion etching [oxygen, 40 SCCM (standard cubic centimeter per minute); power, 250 W] was performed for 8 hours to etch through the polyimide. The shadow mask was therefore completed and peeled off from the PDMS adhesive. The detailed process is described in the Supplementary Materials.

Cu, IGZO, and MgO thin-membrane preparation

The preparation of Cu, IGZO, and MgO thin membranes involved direct deposition of material onto a polyanhydride substrate through shadow masks. Cu and MgO were deposited by e-beam evaporation, and IGZO was formed by dc sputtering (20 W; 4% of oxygen partial pressure to argon).

Electronic device fabrication

The fabrication of the devices involved multiple materials deposition through shadow masks. The fabrication procedures for the Cu resistor and antenna were the same as those for the Cu and MgO thin membranes described above. The fabrication of the capacitors involved deposition of Cu as the bottom electrode, MgO as the dielectric layer, and Cu as the top electrode onto the polymer sequentially by e-beam evaporator through the shadow masks. The TFTs and logic gates were fabricated by, firstly, depositing 30-nm-thick IGZO on the polyanhydride substrate by dc sputtering (20 W; 4% of oxygen partial pressure to argon) through a shadow mask. Then, the Cu source and drain electrodes, MgO gate dielectric, and Cu gate electrode were formed by e-beam evaporation through the shadow mask. The fabrication of Schottky diodes began with depositing IGZO by dc sputtering through a shadow mask. Ni and Al were deposited by e-beam evaporation with the shadow masks to form the Schottky contact and the ohmic contact, respectively. To fabricate the photodetectors, IGZO was formed by dc sputtering, and the Cu electrode was deposited by e-beam evaporation onto the polymer through shadow masks. The memory device fabrication involved depositing a Cu bottom electrode by e-beam evaporation, an IGZO active layer by dc sputtering, and a Cu top electrode by e-beam evaporation through shadow masks onto the substrate directly. The detailed fabrication procedure is described in the Supplementary Materials.

Material characterization and device measurements

A digital camera (Nikon D7100) and an optical microscope (Nikon LV100) were used to capture the optical images of samples during the triggered transience. The FTIR was recorded by a Vector 22 FTIR spectrometer. The electrical characteristics of all the devices were measured using a sourcemeter (Keithley 2400). It is noted that the polymer substrates are very sensitive to moisture. All the polymer substrates and fabricated transient electronics were stored in a nitrogen-filled glove box at a relative humidity of 0%.

SUPPLEMENTARY MATERIALS

Supplementary material for this article is available at http://advances.sciencemag.org/cgi/content/full/3/9/e1701222/DC1

Synthesis scheme of the humidity-controlled degradable polymer
Preparation scheme of shadow masks
Preparation scheme of the metal and oxide membranes onto the polymer
Fabrication of the Cu resistor and antenna onto the polymer
Fabrication of the capacitor onto the polymer
Fabrication of the field-effect transistor and inverter onto the polymer
Fabrication of the Schottky diode onto the polymer
Fabrication of the UV detector onto the polymer
Fabrication of the resistive memory onto the polymer
Tuning of components in the polymer preparation
Characterization of the resistor
Characterization of the antenna
Characterization of the capacitor
Characterization of the TFT
Characterization of the inverter
Characterization of the Schottky diode
Characterization of the photodetector
Characterization of the resistive memory device
table S1. Precursors for polyanhydride films with different compositions (the calculation depends on the PEG molar ratio in the mixture).
fig. S1. An optical image of the cross section of the polyanhydride substrate.
fig. S2. The transmittance spectrum of a moisture-sensitive polyanhydride thin film in visible range.
fig. S3. The time-sequential measurements of the FTIR spectra of the polymer thin films during the hydrolysis process under different relative humidity levels.
fig. S4. Optical images showing the time-sequential hydrolysis of the polymer with different compositions of PEG from 0 to 50% at a relative humidity of 90%.

fig. S5. Optical images showing the time-sequential hydrolysis of the polymer with different compositions of PEG from 0 to 50% at a relative humidity of 45%.
fig. S6. Optical images showing the time-sequential hydrolysis of the polymer with different compositions of PEG from 0 to 50% at a relative humidity of 0%.
fig. S7. Optical images showing the time-sequential hydrolysis of the polymer substrates with different film thicknesses under different relative humidity levels.
fig. S8. Cu antenna.
fig. S9. MgO-based capacitor.
fig. S10. IGZO-based TFT.
fig. S11. Logic gate inverter.
fig. S12. IGZO-based diode.
fig. S13. IGZO-based photodetector.
fig. S14. IGZO-based resistive memory.

REFERENCES AND NOTES

1. S.-W. Hwang, H. Tao, D.-H. Kim, H. Cheng, J.-K. Song, E. Rill, M. A. Brenckle, B. Panilaitis, S. M. Won, Y.-S. Kim, Y. M. Song, K. J. Yu, A. Ameen, R. Li, Y. Su, M. Yang, D. L. Kaplan, M. R. Zakin, M. J. Slepian, Y. Huang, F. G. Omenetto, J. A. Rogers, A physically transient form of silicon electronics. *Science* **337**, 1640–1644 (2012).
2. S.-K. Kang, R. K. J. Murphy, S.-W. Hwang, S. M. Lee, D. V. Harburg, N. A. Krueger, J. Shin, P. Gamble, H. Cheng, S. Yu, Z. Liu, J. G. McCall, M. Stephen, H. Ying, J. Kim, G. Park, R. C. Webb, C. H. Lee, S. Chung, D. S. Wie, A. D. Gujar, B. Vemulapalli, A. H. Kim, K.-M. Lee, J. Cheng, Y. Huang, S. H. Lee, P. V. Braun, W. Z. Ray, J. A. Rogers, Bioresorbable silicon electronic sensors for the brain. *Nature* **530**, 71–76 (2016).
3. H. Tao, S.-W. Hwang, B. Marelli, B. An, J. E. Moreau, M. Yang, M. A. Brenckle, S. Kim, D. L. Kaplan, J. A. Rogers, F. G. Omenetto, Silk-based resorbable electronic devices for remotely controlled therapy and in vivo infection abatement. *Proc. Natl. Acad. Sci. U.S.A.* **111**, 17385–17389 (2014).
4. Y. H. Jung, T.-H. Chang, H. Zhang, C. Yao, Q. Zheng, V. W. Yang, H. Mi, M. Kim, S. J. Cho, D.-W. Park, H. Jiang, J. Lee, Y. Qiu, W. Zhou, Z. Cai, S. Gong, Z. Ma, High-performance green flexible electronics based on biodegradable cellulose nanofibril paper. *Nat. Commun.* **6**, 7170 (2015).
5. K. J. Yu, D. Kuzum, S.-W. Hwang, B. H. Kim, H. Juul, N. H. Kim, S. M. Won, K. Chiang, M. Trumpis, A. G. Richardson, H. Cheng, H. Fang, M. Thompson, H. Bink, D. Talos, K. J. Seo, H. N. Lee, S.-K. Kang, J.-H. Kim, J. Y. Lee, Y. Huang, F. E. Jensen, M. A. Dichter, T. H. Lucas, J. Viventi, B. Litt, J. A. Rogers, Bioresorbable silicon electronics for transient spatiotemporal mapping of electrical activity from the cerebral cortex. *Nat. Mater.* **15**, 782–791 (2016).
6. D. Son, J. Lee, D. J. Lee, R. Ghaffari, S. Yun, S. J. Kim, J. E. Lee, H. R. Cho, S. Yoon, S. Yang, S. Lee, S. Qiao, D. Ling, S. Shin, J.-K. Song, J. Kim, T. Kim, H. Lee, J. Kim, M. Soh, N. Lee, C. S. Hwang, S. Nam, N. Lu, T. Hyeon, S. H. Choi, D.-H. Kim, Bioresorbable electronic stent integrated with therapeutic nanoparticles for endovascular diseases. *ACS Nano* **9**, 5937–5946 (2015).
7. X. Huang, Y. Liu, S.-W. Hwang, S.-K. Kang, D. Patnaik, J. F. Cortes, J. A. Rogers, Biodegradable materials for multilayer transient printed circuit boards. *Adv. Mater.* **26**, 7371–7377 (2014).
8. S. H. Jin, J. Shin, I.-T. Cho, S. Y. Han, D. J. Lee, C. H. Lee, J.-H. Lee, J. A. Rogers, Solution-processed single-walled carbon nanotube field effect transistors and bootstrapped inverters for disintegratable, transient electronics. *Appl. Phys. Lett.* **105**, 013506 (2014).
9. N. Banerjee, Y. Xie, M. M. Rahman, H. Kim, C. H. Mastrangelo, From chips to dust: The MEMS shatter secure chip, in *2014 IEEE 27th International Conference on Micro Electro Mechanical Systems (MEMS)* (IEEE, 2014), pp. 1123–1126.
10. N. Banerjee, Y. Xie, H. Kim, C. H. Mastrangelo, Microfluidic device for triggered chip transience, in *2013 IEEE Sensors* (IEEE, 2013), pp. 1–4.
11. J. Lee, B. Yoo, H. Lee, G. D. Cha, H.-S. Lee, Y. Cho, S. Y. Kim, H. Seo, W. Lee, D. Son, M. Kang, H. M. Kim, Y. I. Park, T. Hyeon, D.-H. Kim, Ultra-wideband multi-dye-sensitized upconverting nanoparticles for information security application. *Adv. Mater.* **29**, 1603169 (2017).
12. C. Dagdeviren, S.-W. Hwang, Y. Su, S. Kim, H. Cheng, O. Gur, R. Haney, F. G. Omenetto, Y. Huang, J. A. Rogers, Transient, biocompatible electronics and energy harvesters based on ZnO. *Small* **9**, 3398–3404 (2013).
13. H. L. Hernandez, S.-K. Kang, O. P. Lee, S.-W. Hwang, J. A. Kaitz, B. Inci, C. W. Park, S. Chung, N. R. Sottos, J. S. Moore, J. A. Rogers, S. R. White, Triggered transience of metastable poly(phthalaldehyde) for transient electronics. *Adv. Mater.* **26**, 7637–7642 (2014).
14. C. W. Park, S.-K. Kang, H. L. Hernandez, J. A. Kaitz, D. S. Wie, J. Shin, O. P. Lee, N. R. Sottos, J. S. Moore, J. A. Rogers, S. R. White, Thermally triggered degradation of transient electronic devices. *Adv. Mater.* **27**, 3783–3788 (2015).
15. S.-W. Hwang, S.-K. Kang, X. Huang, M. A. Brenckle, F. G. Omenetto, J. A. Rogers, Materials for programmed, functional transformation in transient electronic systems. *Adv. Mater.* **27**, 47–52 (2015).
16. S.-W. Hwang, D.-H. Kim, H. Tao, T.-i. Kim, S. Kim, K. J. Yu, B. Panilaitis, J.-W. Jeong, J.-K. Song, F. G. Omenetto, J. A. Rogers, Materials and fabrication processes for transient and bioresorbable high-performance electronics. *Adv. Funct. Mater.* **23**, 4087–4093 (2013).
17. S.-W. Hwang, G. Park, H. Cheng, J.-K. Song, S.-K. Kang, L. Yin, J.-H. Kim, F. G. Omenetto, Y. Huang, K.-M. Lee, J. A. Rogers, 25th anniversary article: Materials for high-performance biodegradable semiconductor devices. *Adv. Mater.* **26**, 1992–2000 (2014).
18. S.-W. Hwang, C. H. Lee, H. Cheng, J.-W. Jeong, S.-K. Kang, J.-H. Kim, J. Shin, J. Yang, Z. Liu, G. A. Ameer, Y. Huang, J. A. Rogers, Biodegradable elastomers and silicon nanomembranes/nanoribbons for stretchable, transient electronics, and biosensors. *Nano Lett.* **15**, 2801–2808 (2015).
19. S.-W. Hwang, G. Park, C. Edwards, E. A. Corbin, S.-K. Kang, H. Cheng, J.-K. Song, J.-H. Kim, S. Yu, J. Ng, J. E. Lee, J. Kim, C. Yee, B. Bhaduri, Y. Su, F. G. Omennetto, Y. Huang, R. Bashir, L. Goddard, G. Popescu, K.-M. Lee, J. A. Rogers, Dissolution chemistry and biocompatibility of single-crystalline silicon nanomembranes and associated materials for transient electronics. *ACS Nano* **8**, 5843–5851 (2014).
20. S.-K. Kang, S.-W. Hwang, H. Cheng, S. Yu, B. H. Kim, J.-H. Kim, Y. Huang, J. A. Rogers, Dissolution behaviors and applications of silicon oxides and nitrides in transient electronics. *Adv. Funct. Mater.* **24**, 4427–4434 (2014).
21. C. J. Bettinger, Z. Bao, Organic thin-film transistors fabricated on resorbable biomaterial substrates. *Adv. Mater.* **22**, 651–655 (2010).
22. S.-W. Hwang, J.-K. Song, X. Huang, H. Cheng, S.-K. Kang, B. H. Kim, J.-H. Kim, S. Yu, Y. Huang, J. A. Rogers, High-performance biodegradable/transient electronics on biodegradable polymers. *Adv. Mater.* **26**, 3905–3911 (2014).
23. L. Yin, A. B. Farimani, K. Min, N. Vishal, J. Lam, Y. K. Lee, N. R. Aluru, J. A. Rogers, Mechanisms for hydrolysis of silicon nanomembranes as used in bioresorbable electronics. *Adv. Mater.* **27**, 1857–1864 (2015).
24. L. Yin, H. Cheng, S. Mao, R. Haasch, Y. Liu, X. Xie, S.-W. Hwang, H. Jain, S.-K. Kang, Y. Su, R. Li, Y. Huang, J. A. Rogers, Dissolvable metals for transient electronics. *Adv. Funct. Mater.* **24**, 645–658 (2014).
25. H. Acar, S. Çinar, M. Thunga, M. R. Kessler, N. Hashemi, R. Montazami, Study of physically transient insulating materials as a potential platform for transient electronics and bioelectronics. *Adv. Funct. Mater.* **24**, 4135–4143 (2014).
26. A. Gopferich, J. Tessmar, Polyanhydride degradation and erosion. *Adv. Drug Deliv. Rev.* **54**, 911–931 (2002).
27. H. B. Rosen, J. Chang, G. E. Wnek, R. J. Linhardt, R. Langer, Bioerodible polyanhydrides for controlled drug delivery. *Biomaterials* **4**, 131–133 (1983).
28. D.-H. Kim, Y.-S. Kim, J. Amsden, B. Panilaitis, D. L. Kaplan, F. G. Omenetto, M. R. Zakin, J. A. Rogers, Silicon electronics on silk as a path to bioresorbable, implantable devices. *Appl. Phys. Lett.* **95**, 133701 (2009).
29. P.-T. Liu, Y.-T. Chou, L.-F. Teng, F.-H. Li, H.-P. Shieh, Nitrogenated amorphous InGaZnO thin film transistor. *Appl. Phys. Lett.* **98**, 052102 (2011).
30. T. H. Chang, C. J. Chiu, S. J. Chang, T. Y. Tsai, T. H. Yang, Z. D. Huang, W. Y. Weng, Amorphous InGaZnO ultraviolet phototransistors with double-stack Ga_2O_3/SiO_2 dielectric. *Appl. Phys. Lett.* **102**, 221104 (2013).
31. B. G. Baker, B. B. Johnson, G. L. C. Maire, Photoelectric work function measurements on nickel crystals and films. *Surf. Sci.* **24**, 572–586 (1971).
32. S. Miyazaki, Photoemission study of energy-band alignments and gap-state density distributions for high-k gate dielectrics. *J. Vac. Sci. Technol. B Microelectron. Nanometer Struct. Process. Meas. Phenom.* **19**, 2212–2216 (2001).

Acknowledgments: We thank the facility support from the University of Houston Nanofabrication Facility and the University of Science and Technology of China (USTC) Center for Micro- and Nanoscale Research and Fabrication. C.Y. also would like to thank J. Zhang and L. Chang for providing help on equipment. **Funding:** H.X. acknowledges funding support from the National Key Basic Research Program of China (2015CB351903), National Natural Science Foundation of China (grant numbers 51402282 and 21474095), and the Fundamental Research Funds for the Central Universities. C.Y. would like to acknowledge partial financial support from the NSF (ECCS-1509763 and CMMI-1554499) and the Doctoral New Investigator grant from the American Chemical Society Petroleum Research Fund, as well as Bill D. Cook Faculty Scholarship support from the University of Houston. **Author contributions:** Y.G., Y.Z., X.W., K.S., H.X., and C.Y. conceived and designed the experiments. Y.G., Y.Z., X.W., and K.S. performed the experiments. Y.G., Y.Z., X.W., K.S., H.X., C.Y., J.L., J.C., and X.Y. analyzed the data. Y.G., Y.Z., X.W., K.S., H.X., and C.Y. wrote the manuscript. **Competing interests:** The authors declare that they have no competing interests. **Data and materials availability:** All data needed to evaluate the conclusions in the paper are present in the paper and/or the Supplementary Materials. Additional data related to this paper may be requested from the authors.

Submitted 17 April 2017
Accepted 8 August 2017
Published 1 September 2017
10.1126/sciadv.1701222

Citation: Y. Gao, Y. Zhang, X. Wang, K. Sim, J. Liu, J. Chen, X. Feng, H. Xu, C. Yu, Moisture-triggered physically transient electronics. *Sci. Adv.* **3**, e1701222 (2017).

Science Advances

Moisture-triggered physically transient electronics

Yang Gao, Ying Zhang, Xu Wang, Kyoseung Sim, Jingshen Liu, Ji Chen, Xue Feng, Hangxun Xu and Cunjiang Yu

Sci Adv **3** (9), e1701222.
DOI: 10.1126/sciadv.1701222